Title

Differential effects of myostatin deficiency on motor and sensory axons

Journal

Muscle & Nerve, 56(6)

ISSN

0148-639X

Authors

Jones, Maria R
Villalón, Eric
Northcutt, Adam J
et al.

Publication Date

2017-12-01

DOI

10.1002/mus.25570

Peer reviewed

HHS Public Access

Author manuscript

Muscle Nerve. Author manuscript; available in PMC 2018 December 01.

Published in final edited form as:

Muscle Nerve. 2017 December ; 56(6): E100–E107. doi:10.1002/mus.25570.

Differential effects of myostatin deficiency on motor and sensory axons

Maria R. Jones, Ph.D.[1,2], **Eric Villalón, Ph.D.**[1,2], **Adam J. Northcutt, B.S.**[1], **Nigel A. Calcutt, Ph.D.**[3], and **Michael L. Garcia, Ph.D.**[1,2,*]

[1]Department of Biological Sciences, University of Missouri, Columbia, MO 65211

[2]C.S. Bond Life Sciences Center, University of Missouri, Columbia, MO 65211

[3]Department of Pathology, University of California San Diego, La Jolla, CA 92093

Abstract

Introduction—Deletion of myostatin in mice (*MSTN*$^{-/-}$) alters structural properties of peripheral axons. However, properties like axon diameter and myelin thickness were analyzed in mixed nerves, so it is unclear if loss of myostatin affects motor, sensory or both types of axons.

Methods—Using the *MSTN*$^{-/-}$ mouse model, we analyzed the effects of increasing the number of muscle fibers on axon diameter, myelin thickness, and internode length in motor and sensory axons.

Results—Axon diameter and myelin thickness were increased in motor axons of *MSTN*$^{-/-}$ mice without affecting internode length or axon number. The number of sensory axons was increased without affecting their structural properties.

Discussion—These results suggest that motor and sensory axons establish structural properties by independent mechanisms. Moreover, in motor axons, instructive cues from the neuromuscular junction may play a role in co-regulating axon diameter and myelin thickness, while internode length is established independently.

Keywords

axon diameter; myelin thickness; nerve conduction velocity; internode length; innervation field; myostatin deficiency

Introduction

Rapid impulse propagation allows complex nervous systems to operate quickly and efficiently. Three structural properties are maximized to ensure rapid impulse propagation: axonal diameter, myelin sheath thickness, and internode length. These properties are

*To whom correspondence should be addressed: Michael L. Garcia, University of Missouri, 340C C.S. Bond Life Sciences Center, 1201 E Rollins Rd., Columbia, MO 65211, Phone: 573-882-9712, GarciaML@missouri.edu.

Ethical Publication: We confirm that we have read the Journal's position on issues involved in ethical publication and affirm that this report is consistent with those guidelines.

Conflict Disclosure: None of the authors has any conflict of interest to disclose.

regulated by different molecular mechanisms, but all 3 are interrelated. Establishing axon diameter occurs through myelin-dependent radial axonal growth[1, 2] and neurofilament accumulation[3, 4]. Neurofilament composition varies with age[5, 6] and location in the nervous system[7, 8]. However, following postnatal development, all neurofilaments are composed of a common core of subunit proteins, neurofilament light (NF-L), medium (NF-M), and heavy (NF-H), that form obligate heteropolymers[9]. Gene targeting studies identified NF-M as the critical subunit[10] and NF-M Carboxy-terminus (C-terminus) as the critical domain for radial axonal growth[11, 12]. The overall length of the NF-M C-terminus appears to be important in determining axon diameter[12]. However, the precise mechanism by which the length of NF-M C-terminus establishes axon diameter remains unclear.

Expansion of axonal diameter accompanied by myelination increases conduction velocity at a greater rate than expanding axonal diameter alone above a critical threshold[13, 14]. The critical diameter for myelination is 1 μm[15]. However, it is not diameter *per se* that instructs Schwann cells to myelinate. Axonal levels of neuregulin 1 type III (NRG1 Type III) define which axons are fated for myelination[16]. Axons expressing NRG1 Type III above a threshold will become myelinated[17]. Moreover, myelin thickness is also determined by axonal NRG1 Type III levels[18].

The length of the myelinating Schwann cell defines internode length and is critical for defining conduction velocity in myelinated fibers. Reducing internode length reduces nerve conduction velocity[19]. It has been known for over 140 years that internode length positively correlates with axon diameter[20], and several proteins have been identified that can influence internode length. However, it is unclear how the correlation between internode length and axon diameter is initially established.

Genetic alteration of a single structural property does not result in compensatory changes in the remaining properties. Increased expression of NRG1 Type III resulted in thicker myelin without increasing axon diameter[18] while increasing axon diameter did not result in thicker myelin[12]. Reducing the number of superior cervical ganglion axons innervating the submandibular salivary gland in rats increased axon diameter and induced myelination[21]. Manipulating relative target size in rats altered the composition of sympathetic postganglionic axons from primarily small unmyelinated axons to primarily large myelinated axons[21]. Muscle hyperplasia, due to deletion of myostatin[22], also increased diameter and myelin thickness of axons within sciatic and radial nerves[23]. However, it was unclear if motor, sensory, or both axon types were altered.

Taken together, these studies suggest that interactions with target tissue may contribute to axonal growth. Prior studies have observed that myostatin deficient mice have a larger innervation ratio[24], where peripheral nervous system (PNS) motor axons innervate a larger proportion of muscle fibers relative to wild type mice. In this study, we utilized the myostatin deficient mouse model to test the effect of muscle hyperplasia on total axon number, as well as structural properties of PNS sensory and motor axons.

Methods

Animals

All procedures were in compliance with the University of Missouri Animal Care and Use Committee and with all local and federal laws governing the humane treatment of animals. Mice housed in cages (up to 5 mice per cage) on a 12-h light/dark cycle and were given food and water *ad libitum*. *MSTN*$^{-/-}$ were a generous gift from Se-Jin Lee (Johns Hopkins University), and were maintained on a C57Bl/6 background. *MSTN*$^{-/-}$ and *MSTN*$^{+/+}$ were produced from homozygous matings. All mice used in these experiments were 1-month old, as 1-month-old myostation null mice do not show any signs of muscle damage[22].

Tissue preparation, axon morphological analysis

Mice were sacrificed, and 5th lumbar roots were dissected immediately. One root was fixed for axon diameter and myelin analysis, while the other was fixed for teased fiber analysis, as described below. Histological and nerve conduction velocity analyses were performed on unique cohorts of mice.

Axon diameter and myelin analysis—Fifth lumbar (L5) spinal roots were post-fixed in 2.5% glutaraldehyde and 4% paraformaldehyde in 0.1 M Sorenson phosphate buffer, pH 7.2 overnight. L5 roots were subsequently treated with 2% osmium tetroxide, washed, dehydrated, and embedded in Epon-Araldite resin. Thick sections (0.75 μm) for light microscopy were stained with ρ-phenylenediamine. Images of cross sections of L5 motor axons were collected with a Zeiss Axio Imager A1 light microscope (Carl Zeiss MicroImaging GmbH, Jena, Germany). Cross sections of L5 motor and sensory roots were analyzed in 3 mice per genotype. Entire roots were imaged, imaging thresholds were selected individually, and the cross-sectional area of each axon was calculated and reported as the diameter of a circle of equivalent area using the Image J Software (National Institutes of Health). Axon diameters were grouped into 0.5 μm bins. For axon diameters and total axon number, every axon in the root was measured (~1000 for motor roots, ~2600 for sensory roots). Myelin thickness and *g*-ratios were estimated by measuring the axonal diameter and fiber diameter of individual axons for 10% of all axons per motor roots using Image J. For myelin thickness and g-ratio, ~10% of axons in the root were analyzed (n=449, 408 motor +/+ and −/−; n=750, 751 sensory +/+ and −/−). The total number of axons was analyzed for statistical significance by unpaired *t*-tests (SigmaPlot, Systat Software, Inc.). Distributions of motor axon diameter, myelin thickness, and g-ratio were not normally distributed, and were thus analyzed for statistical significance by a Mann–Whitney Rank Sum test (SigmaPlot, Systat Software, Inc.).

Teased fiber analysis—L5 roots were immersion fixed in a 2.5 M glutaraldehyde, 0.025 M sodium cacodylate, pH 7.38 solution for 25 min at 4°C, rinsed in 1X PBS for 5 minutes and transferred to a saturated solution of Sudan black in 70% ethanol and allowed to incubate for 1 hour at room temperature. Tissue samples were then rinsed twice in 70% ethanol for 5 minutes and transferred to a 10% glycerin solution. Fifty to 100 axon bundles were separated from the ventral L5 root. The bundle was transferred to a super frost microscope slide containing a thin layer of a 10% aqueous solution of glycerin:BSA (1:1).

Individual fibers were teased apart from the bundle and laid out on the glass slide. Fibers were then allowed to dry overnight on a 50°C hot plate. Digital photos of the fibers were taken using the AxioVision Digital Image Processing Software (Carl Zeiss MicroImaging). Internode lengths were measured using ImageJ (NIH). At least 200 internodes were measured from each tissue sample, and at least 3 animals were used per genotype. An average of the internode lengths for each genotype was calculated and tested for statistical significance by unpaired *t*-tests (SigmaPlot, Systat Software, Inc.). Internode length was also compared to total fiber diameter, with fiber diameter measured at 10 evenly spaced intervals and averaged per internode. Fiber diameter at internodes was also compared for statistical significance by unpaired *t*-tests (SigmaPlot, Systat Software, Inc.).

Nerve conduction velocity measurements

Nerve conduction velocities were measured in the sciatic nerve, interosseus muscle system[25]. In brief, mice were anesthetized with isoflurane, and core temperature was maintained at 37°C by a thermal pad and monitored with a rectal thermometer. The sciatic nerve was stimulated with single supramaximal square wave pulses (3 V and 0.05 ms duration) via fine needle electrodes placed at the sciatic notch and Achilles tendon. Evoked electromyograms were recorded from the interosseus muscles of the ipsilateral foot via 2 fine needle electrodes and displayed on a digital storage oscilloscope. The distance between the 2 stimulation sites was measured using calipers, and conduction velocity was calculated by taking the distance between the 2 sites divided by the time difference between the M wave peaks at each site. Measurements were made in triplicate from a minimum of 5 animals per genotype, and the median was used as the measure of velocity. Values were compared for statistical significance by an unpaired *t*-test (SigmaPlot, Systat Software, Inc.).

Results

Myostatin deficiency results in increased axon diameter in motor axons

Fifth lumbar (L5) motor roots were imaged and analyzed from both myostatin wild type ($MSTN^{+/+}$) and myostatin deficient ($MSTN^{-/-}$) mice (Fig. 1A). $MSTN^{-/-}$ mice had a similar total number of axons in the L5 motor root when compared with $MSTN^{+/+}$ (Fig. 1B). Motor axons displayed the typical bimodal distribution in both $MSTN^{+/+}$ and $MSTN^{-/-}$ mice (Fig. 1C and 1D). Small diameter axons represent gamma motor neurons[26, 27], and large diameter axons represent alpha motor neurons[26]. Peak diameter for $MSTN^{-/-}$ gamma motor axons was increased relative to $MSTN^{+/+}$ gamma motor axons (Fig. 1C). Peak diameter was also increased in $MSTN^{-/-}$ alpha motor axons (Fig. 1C). Statistical analysis of the motor distributions showed differences in all between $MSTN^{+/+}$and $MSTN^{-/-}$ (Fig. 1D). The increase in the median diameter in $MSTN^{-/-}$ was statistically significant by a Mann Whitney U test ($P<0.001$).

Alpha and gamma motor neuron populations were estimated for $MSTN^{-/-}$ and $MSTN^{+/+}$ mice by binning total numbers using the lowest point between the 2 peaks as the cutoff (Table 1). There was a significant reduction in total number of putative gamma motor neurons in $MSTN^{-/-}$ mice compared to $MSTN^{+/+}$ mice ($P=0.022$), while alpha motor neurons were not different between the 2 groups (Fig. 2).

Sensory axons show similar diameter distributions, but demonstrate an increase in total axon number

L5 sensory roots were imaged and analyzed for both *MSTN*$^{+/+}$ and *MSTN*$^{-/-}$ mice (Fig. 3A). Total number of sensory axons was significantly increased in *MSTN*$^{-/-}$ mice (Fig. 3B). Diameter distributions were determined for all sensory axons in *MSTN*$^{+/+}$ and *MSTN*$^{-/-}$ mice (Fig. 3C and 3D). Sensory axon profiles were unimodal for both *MSTN*$^{+/+}$ and *MSTN*$^{-/-}$ mice (Fig. 3C). Peak diameter was not changed in sensory axons, but statistical analysis showed very similar distributions in all quartiles.

The number of 1–1.5 μm axons was significantly increased in *MSTN*$^{-/-}$ mice (791±45) compared to *MSTN*$^{+/+}$ mice (608±44) when analyzed by the student *t*-test (P=0.023), although no other point showed differences. Binning to estimate small vs large diameter sensory axons identified an overall trend towards a greater number of axons in *MSTN*$^{-/-}$ mice that did not reach statistical significance (Table 1).

Myelin thickness is increased in motor axons, but not sensory axons

Myelin thickness was measured and g-ratio was calculated in 10% of motor (Fig. 4) and sensory (Fig. 5) axons in the L5 motor and sensory roots. Analysis of motor axon myelin suggested an increase in myelin thickness in *MSTN*$^{-/-}$ mice relative to axonal diameter (Fig. 4A). Median myelin thickness of axons in *MSTN*$^{-/-}$ mice was increased from 0.75 μm in *MSTN*$^{+/+}$ to 1.13 μm in *MSTN*$^{-/-}$ (P<0.001). Increased myelin thickness (Fig. 4) coupled with increased axon diameter (Fig. 1) in *MSTN*$^{-/-}$ mice predicts a similar g-ratio for *MSTN*$^{+/+}$ and *MSTN*$^{-/-}$ mice. However, the g-ratio of *MSTN*$^{-/-}$ was significantly (P=0.03) decreased compared to that of *MSTN*$^{+/+}$ mice (Fig. 4C, D), suggesting that myelin was disproportionately thick in *MSTN*$^{-/-}$ mice.

Myelin thickness and g-ratio of sensory axons from *MSTN*$^{-/-}$ mice were similar to those from *MSTN*$^{+/+}$ mice except for the largest sensory axons (Fig. 5). For the largest sensory axons, myelin was thinner in *MSTN*$^{-/-}$ mice (Fig. 5A) resulting in an increased g-ratio (Fig. 5C), but values were not significantly different for the population as a whole (Fig. 5B,D).

Internode length is not altered in myostatin deficient mice, although total fiber diameter is increased

Internode length was analyzed in L5 large motor axons by teased fiber analysis. Average internode length was not different in *MSTN*$^{-/-}$ compared to *MSTN*$^{+/+}$ mice (Fig. 6A). To compare internode length to fiber diameter, fiber diameter was measured in 20% of the internodes. Average fiber diameter was significantly increased (P<0.001) in *MSTN*$^{-/-}$ internodes (7.67±0.07 μm) compared to *MSTN*$^{+/+}$ internodes (6.15±0.05 μm) (Fig 6B). This increased diameter corresponded well with the increase measured in cross sections (Fig 1C). Internode length was compared to average fiber diameter per internode (Fig. 6C). This analysis revealed that internode length was not increased in *MSTN*$^{-/-}$ axons. Given the positive correlation between axon diameter and internode length[20], internode length was predicted to be increased to maintain optimal nerve conduction[28]. For example, internode lengths of 400–800 μm were measured on axons that were 6 μm in diameter from *MSTN*$^{+/+}$

mice. However, in *MSTN*$^{-/-}$ mice, this range of internode lengths was observed on axons that were nearly 8 μm in diameter.

Nerve conduction velocity is not different in myostatin deficient mice

To determine if the observed structural alterations affected nerve function, nerve conduction velocity (NCV) was measured in motor axons of the sciatic nerve. NCV tended to be slower in *MSTN*$^{-/-}$ mice compared to *MSTN*$^{+/+}$ mice but this difference did not reach statistical significance (Fig. 7).

Discussion

During postnatal development, 3 key structural properties are established that enhance the speed of neuronal transmission: axon diameter, myelin thickness, and internode length. Genetic manipulation of individual molecular determinants of axon diameter and myelin thickness suggested that, once established, plasticity is not maintained, as altering 1 structural property did not result in compensatory changes in the remaining properties[12, 18]. Altering innervation field size either surgically[21] or genetically in the myostatin deficient mouse[23] increases axon diameter and myelin thickness. However, prior experiments using *MSTN*$^{-/-}$ mice examined axon diameter and myelin thickness in mixed nerves[23] and could not separate motor vs sensory phenotypes. Our study has identified sub-type specific diversity in neuronal structure in response to increased number of muscle fibers, as demonstrated by an increase in axon diameter and myelin thickness in motor axons but an increased total axon number in sensory axons.

Mechanistically, it is unclear how muscle hypertrophy exerts differential effects on different axon types. For motor neurons, a possibility is the distal structure of the axons. Motor axons form neuromuscular junctions with targets. In drosophila, presynaptic metabotropic glutamate receptors (DmGluRA) regulate motor axon diameter through activation of Phosphoinositide 3-kinase (PI3K) through a calcium/calmodulin dependent kinase II and Drosophila Focal Adhesion Kinase dependent mechanism[29, 30]. An analogous system is present at the mammalian neuromuscular junction. The M2 muscarinic acetylcholine receptor (mAchR) is also present on presynaptic terminals of vertebrate neuromuscular junctions[31, 32]. Interestingly, M2 mAchRs share many similarities with DmGluRA, and both are classified as inhibitory G protein-coupled receptors[31] that reduce neuronal excitability[33]. Inhibition of M2 mAchR[32] and DmGluRA[29] leads to a reduction in nerve terminals. Finally, activation of M2 mAchR increases intracellular calcium, suggesting a possible link to calcium-calmodulin dependent kinase II activity. While studies from drosophila have provided potential insights, it is unclear whether autocrine activation of M2 mAchRs specifically regulates molecular determinants of axon diameter or myelin thickness.

Structural properties of gamma motor neurons were increased similarly to alpha motor neurons. Increased axon diameter and myelin thickness could be a result of the increase in muscle spindles observed in *MSTN*$^{-/-}$ mice[23]. However, the number of gamma motor neurons was reduced. It is possible that the overall number was lower without actual loss of gamma motor neurons. Axon diameter was increased in alpha motor neurons by ~1μm. If gamma motor neurons had the same magnitude of response, then their diameters would have

become ~2μm, which placed them within the diameter range that we classified as alpha motor neurons. Though the increase was not significant, we observed a small increase in the number of alpha motor neurons.

Unlike motor axons, sensory axon structural properties were unaffected in *MSTN*$^{-/-}$ mice. Instead, we observed an increase in the total number of sensory axons. Smaller sensory axons are free nerve endings in smaller unmyelinated (C-fibers) or myelinated (A delta or Aδ) axons[34, 35]. Based on our results, we observed the largest difference of total sensory axon number in small myelinated axons, which corresponds to an increase in Aδ axons. Aδ fibers respond to noxious stimuli in the skin[34, 35]. Mechanistically, it is possible that more Aδ fibers were a direct result of muscle hyperplasia and hypertrophy in *MSTN*$^{-/-}$ mice. Muscle hyperplasia and hypertrophy likely increased the skin surface area, resulting in an increased number of Aδ fibers. We would also predict that increased skin surface area would increase C-fibers as well. However, our analysis was limited to myelinated axons.

Internode length positively correlates with axon diameter[20]. Our analysis suggests that internode length was established independently of axon diameter and myelin thickness. Several genes have been identified that influence internode length[19, 36–39], but none of them provide clear mechanistic insight into how the correlation is established or maintained. A possible link between axon diameter and internode length might be neurofilament proteins. Neurofilaments are required for determining axon diameter[3, 40, 41], and the medium and heavy subunit proteins are phosphorylated in a myelin-dependent manner[2, 42]. Further, Schwann cell-specific deletion of mammalian target of rapamycin (mTor) reduced internode length, which correlated with reduced neurofilament phosphorylation[43]. Linking internode length to neurofilaments, perhaps through myelin-dependent phosphorylation, could explain the lack of effect of innervation field size and provide a mechanism for correlating internode length with axon diameter.

Analysis of structural properties involved in regulating neuronal conduction velocity suggests that the size of the innervation field may provide instructive cues for motor axons when establishing axon diameter and myelin thickness, and further exploration of neuromuscular cues is crucial in determining proper establishment of these structural properties.

Acknowledgments

We are thankful to Dr. Se-Jin Lee (Johns Hopkins University) for his generous gift of the myostatin deficient mice. This work was supported by grants from the National Institutes of Health [grant number NS060073], Charcot-Marie-Tooth Association [grant number C00014627], and Missouri Spinal Cord Injury/Disease Research Program to MLG and NS081082 to NAC. Salary support for MLG was provided by the University of Missouri and the C.S. Bond Life Science Center. MRJ was supported by the C. S. Bond Life Sciences Fellowship Program. EV and AJN were supported by a training grants to Dr. Mark Hannink [grant numbers R25 GM056901; and 5T32GM008396].

Abbreviations

C-terminus	Carboxy-terminus
DmGluRA	Drosophila melanogaster metabotropic glutamate receptor

L5	Fifth Lumbar
MSTN	Myostatin
mTor	Mammalian target of rapamycin
NRG	Neuregulin
NF-L	Neurofilament light
NF-M	Neurofilament medium
NF-H	Neurofilament heavy
PI3K	Phosphoinositide 3-kinase
PNS	Peripheral Nervous System

References

1. Lee MK, Cleveland DW. Neuronal intermediate filaments. Annu Rev Neurosci. 1996; 19:187–217. [PubMed: 8833441]
2. de Waegh SM, Lee VM, Brady ST. Local modulation of neurofilament phosphorylation, axonal caliber, and slow axonal transport by myelinating Schwann cells. Cell. 1992; 68(3):451–63. [PubMed: 1371237]
3. Zhu Q, Couillard-Despres S, Julien JP. Delayed maturation of regenerating myelinated axons in mice lacking neurofilaments. Exp Neurol. 1997; 148(1):299–316. [PubMed: 9398473]
4. Ohara O, Gahara Y, Miyake T, Teraoka H, Kitamura T. Neurofilament deficiency in quail caused by nonsense mutation in neurofilament-L gene. J Cell Biol. 1993; 121(2):387–95. [PubMed: 8468353]
5. Shaw G, Weber K. Differential expression of neurofilament triplet proteins in brain development. Nature. 1982; 298(5871):277–9. [PubMed: 7045694]
6. Shen H, Barry DM, Garcia ML. Distal to proximal development of peripheral nerves requires the expression of neurofilament heavy. Neuroscience. 2010; 170(1):16–21. [PubMed: 20633607]
7. Yuan A, Rao MV, Sasaki T, Chen Y, Kumar A, Veeranna, et al. Alpha-internexin is structurally and functionally associated with the neurofilament triplet proteins in the mature CNS. J Neurosci. 2006; 26(39):10006–19. [PubMed: 17005864]
8. Yuan A, Sasaki T, Kumar A, Peterhoff CM, Rao MV, Liem RK, et al. Peripherin is a subunit of peripheral nerve neurofilaments: implications for differential vulnerability of CNS and peripheral nervous system axons. J Neurosci. 2012; 32(25):8501–8. [PubMed: 22723690]
9. Lee MK, Xu Z, Wong PC, Cleveland DW. Neurofilaments are obligate heteropolymers in vivo. J Cell Biol. 1993; 122(6):1337–50. [PubMed: 8376466]
10. Elder GA, Friedrich VL Jr, Bosco P, Kang C, Gourov A, Tu PH, et al. Absence of the mid-sized neurofilament subunit decreases axonal calibers, levels of light neurofilament (NF-L), and neurofilament content. J Cell Biol. 1998; 141(3):727–39. [PubMed: 9566972]
11. Garcia ML, Lobsiger CS, Shah SB, Deerinck TJ, Crum J, Young D, et al. NF-M is an essential target for the myelin-directed “outside-in” signaling cascade that mediates radial axonal growth. J Cell Biol. 2003; 163(5):1011–20. [PubMed: 14662745]
12. Barry DM, Stevenson W, Bober BG, Wiese PJ, Dale JM, Barry GS, et al. Expansion of neurofilament medium C terminus increases axonal diameter independent of increases in conduction velocity or myelin thickness. J Neurosci. 2012; 32(18):6209–19. [PubMed: 22553027]
13. Pumphrey RJ, Young JZ. The rates of conduction of fibres of various diameters in cephalopods. Journal of experimental biology. 1938; 15:453–66.
14. Gasser HS, Grundfest H. Axon Diameters in Relation to the Spike Dimensions and the Conduction Velocity in Mammalian Fibers. American Journal of Physiology. 1939; 127:393–414.

15. Duncan D. A relationship between axone diameter and myelination determined by measurement of myelinated spinal root fibers. J Comp Neurol. 1934; 60:437–71.
16. Nave KA, Salzer JL. Axonal regulation of myelination by neuregulin 1. Curr Opin Neurobiol. 2006; 16(5):492–500. [PubMed: 16962312]
17. Taveggia C, Zanazzi G, Petrylak A, Yano H, Rosenbluth J, Einheber S, et al. Neuregulin-1 type III determines the ensheathment fate of axons. Neuron. 2005; 47(5):681–94. [PubMed: 16129398]
18. Michailov GV, Sereda MW, Brinkmann BG, Fischer TM, Haug B, Birchmeier C, et al. Axonal neuregulin-1 regulates myelin sheath thickness. Science. 2004; 304(5671):700–3. [PubMed: 15044753]
19. Court FA, Sherman DL, Pratt T, Garry EM, Ribchester RR, Cottrell DF, et al. Restricted growth of Schwann cells lacking Cajal bands slows conduction in myelinated nerves. Nature. 2004; 431(7005):191–5. [PubMed: 15356632]
20. Key, A., Retzius, MG. Studien in der Anatomie des Nervensystems und des Bindegewebes. Stockholm: Samson & Wallin; 1876.
21. Voyvodic JT. Target size regulates calibre and myelination of sympathetic axons. Nature. 1989; 342(6248):430–3. [PubMed: 2586612]
22. McPherron AC, Lawler AM, Lee SJ. Regulation of skeletal muscle mass in mice by a new TGF-beta superfamily member. Nature. 1997; 387(6628):83–90. [PubMed: 9139826]
23. Elashry MI, Otto A, Matsakas A, El-Morsy SE, Jones L, Anderson B, et al. Axon and muscle spindle hyperplasia in the myostatin null mouse. J Anat. 2011; 218(2):173–84. [PubMed: 21208206]
24. Gay S, Jublanc E, Bonnieu A, Bacou F. Myostatin deficiency is associated with an increase in number of total axons and motor axons innervating mouse tibialis anterior muscle. Muscle Nerve. 2012; 45(5):698–704. [PubMed: 22499097]
25. Calcutt NA, Tomlinson DR, Biswas S. Coexistence of nerve conduction deficit with increased Na(+)-K(+)-ATPase activity in galactose-fed mice. Implications for polyol pathway and diabetic neuropathy. Diabetes. 1990; 39(6):663–6. [PubMed: 2161366]
26. Kawamura Y, Dyck PJ, Shimono M, Okazaki H, Tateishi J, Doi H. Morphometric comparison of the vulnerability of peripheral motor and sensory neurons in amyotrophic lateral sclerosis. J Neuropathol Exp Neurol. 1981; 40(6):667–75. [PubMed: 7299423]
27. Hunt CC. Relation of function to diameter in afferent fibers of muscle nerves. J Gen Physiol. 1954; 38(1):117–31. [PubMed: 13192320]
28. Brill MH, Waxman SG, Moore JW, Joyner RW. Conduction velocity and spike configuration in myelinated fibres: computed dependence on internode distance. J Neurol Neurosurg Psychiatry. 1977; 40(8):769–74. [PubMed: 925697]
29. Howlett E, Lin CC, Lavery W, Stern M. A PI3-kinase-mediated negative feedback regulates neuronal excitability. PLoS Genet. 2008; 4(11):e1000277. [PubMed: 19043547]
30. Chun-Jen Lin C, Summerville JB, Howlett E, Stern M. The metabotropic glutamate receptor activates the lipid kinase PI3K in Drosophila motor neurons through the calcium/calmodulin-dependent protein kinase II and the nonreceptor tyrosine protein kinase DFak. Genetics. 2011; 188(3):601–13. [PubMed: 21515581]
31. Wess J. Muscarinic acetylcholine receptor knockout mice: novel phenotypes and clinical implications. Annu Rev Pharmacol Toxicol. 2004; 44:423–50. [PubMed: 14744253]
32. Wright MC, Potluri S, Wang X, Dentcheva E, Gautam D, Tessler A, et al. Distinct muscarinic acetylcholine receptor subtypes contribute to stability and growth, but not compensatory plasticity, of neuromuscular synapses. J Neurosci. 2009; 29(47):14942–55. [PubMed: 19940190]
33. Bellingham MC, Berger AJ. Presynaptic depression of excitatory synaptic inputs to rat hypoglossal motoneurons by muscarinic M2 receptors. J Neurophysiol. 1996; 76(6):3758–70. [PubMed: 8985874]
34. Yeomans DC, Proudfit HK. Nociceptive responses to high and low rates of noxious cutaneous heating are mediated by different nociceptors in the rat: electrophysiological evidence. Pain. 1996; 68(1):141–50. [PubMed: 9252009]

35. Yeomans DC, Pirec V, Proudfit HK. Nociceptive responses to high and low rates of noxious cutaneous heating are mediated by different nociceptors in the rat: behavioral evidence. Pain. 1996; 68(1):133–40. [PubMed: 9252008]

36. Court FA, Hewitt JE, Davies K, Patton BL, Uncini A, Wrabetz L, et al. A laminin-2, dystroglycan, utrophin axis is required for compartmentalization and elongation of myelin segments. J Neurosci. 2009; 29(12):3908–19. [PubMed: 19321787]

37. Novak N, Bar V, Sabanay H, Frechter S, Jaegle M, Snapper SB, et al. N-WASP is required for membrane wrapping and myelination by Schwann cells. J Cell Biol. 2011; 192(2):243–50. [PubMed: 21263026]

38. Sherman DL, Wu LM, Grove M, Gillespie CS, Brophy PJ. Drp2 and periaxin form Cajal bands with dystroglycan but have distinct roles in Schwann cell growth. J Neurosci. 2012; 32(27):9419–28. [PubMed: 22764250]

39. Ozcelik M, Cotter L, Jacob C, Pereira JA, Relvas JB, Suter U, et al. Pals1 is a major regulator of the epithelial-like polarization and the extension of the myelin sheath in peripheral nerves. J Neurosci. 2010; 30(11):4120–31. [PubMed: 20237282]

40. Sakaguchi T, Okada M, Kitamura T, Kawasaki K. Reduced diameter and conduction velocity of myelinated fibers in the sciatic nerve of a neurofilament-deficient mutant quail. Neurosci Lett. 1993; 153(1):65–8. [PubMed: 8510825]

41. Eyer J, Peterson A. Neurofilament-deficient axons and perikaryal aggregates in viable transgenic mice expressing a neurofilament-beta-galactosidase fusion protein. Neuron. 1994; 12(2):389–405. [PubMed: 8110465]

42. Hsieh ST, Kidd GJ, Crawford TO, Xu Z, Lin WM, Trapp BD, et al. Regional modulation of neurofilament organization by myelination in normal axons. J Neurosci. 1994; 14(11 Pt 1):6392–401. [PubMed: 7965044]

43. Sherman DL, Krols M, Wu LM, Grove M, Nave KA, Gangloff YG, et al. Arrest of myelination and reduced axon growth when Schwann cells lack mTOR. J Neurosci. 2012; 32(5):1817–25. [PubMed: 22302821]

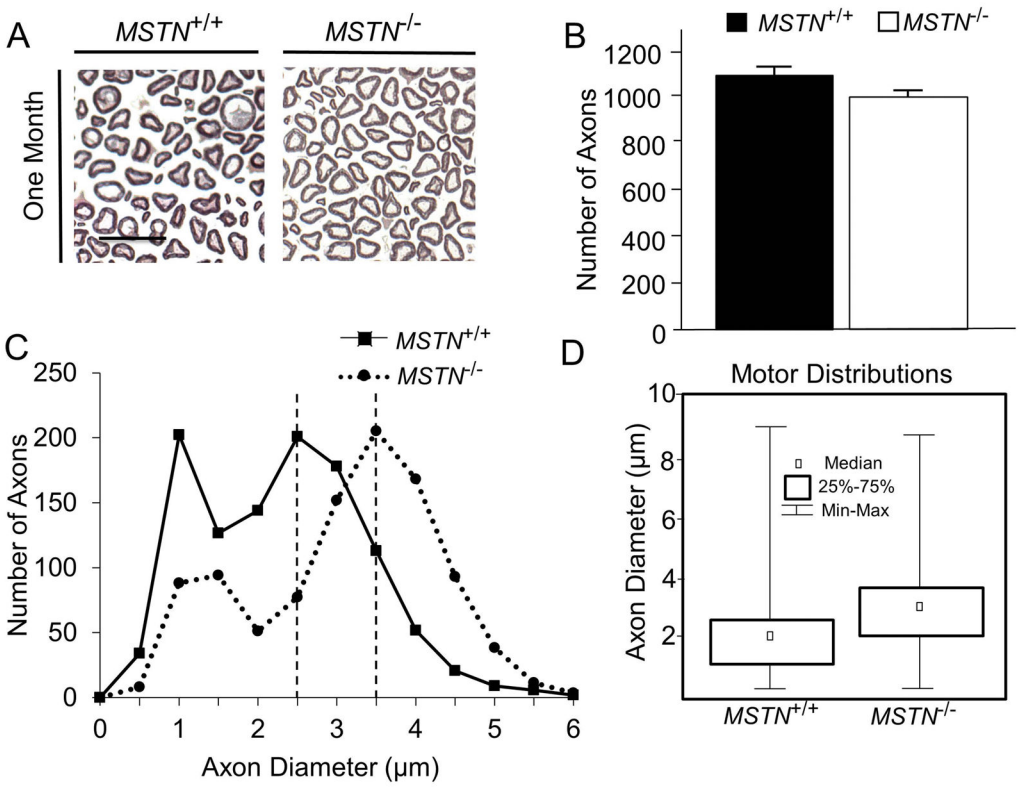

Figure 1. Total numbers and diameters of motor axons in L5 ventral roots of *MSTN*$^{+/+}$ and *MSTN*$^{-/-}$ mice

(A) Cross sections of *MSTN*$^{+/+}$ (left) and *MSTN*$^{-/-}$ mice (right) L5 ventral root axons. Scale bar =10 um. (B) Number of motor axons. Counts were averaged from 3 animals for each genotype and analyzed for statistical significance by unpaired student *t*-test. Means were not significantly different. (C) Distribution of motor axon diameters from *MSTN*$^{+/+}$ and *MSTN*$^{-/-}$ mice. Peak diameters of both small and large diameter axons were larger in *MSTN*$^{-/-}$ mice. Interestingly, the number of small motor axons was reduced in *MSTN*$^{-/-}$ mice. (D) Whisker plots of axonal diameter, showing first, second, and third quartile values for *MSTN*$^{+/+}$ (1.1, 2.1, 2.8 μm respectively) and *MSTN*$^{-/-}$ (2.0, 3.1, 3.7 μm respectively) mice. There was a statistically significant difference between diameter distributions of *MSTN*$^{+/+}$ versus *MSTN*$^{-/-}$ mice (P<0.001: N=3 per genotype).

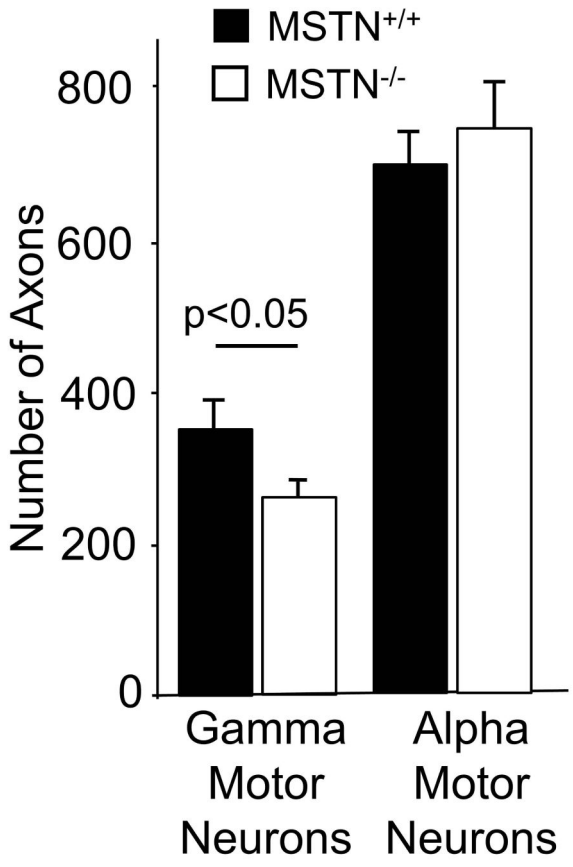

Figure 2. *MSTN*$^{-/-}$ mice demonstrate a decrease in total number of gamma motor neurons

The total number of putative gamma motor neurons was significantly (*P*=0.022: N=3 per genotype) decreased in *MSTN*$^{-/-}$ (242±15) compared to *MSTN*$^{+/+}$ (363±29) mice. There was no difference in putative alpha motor neurons. Total numbers of alpha and gamma motor neurons were analyzed for statistical significance by the student unpaired *t*-test.

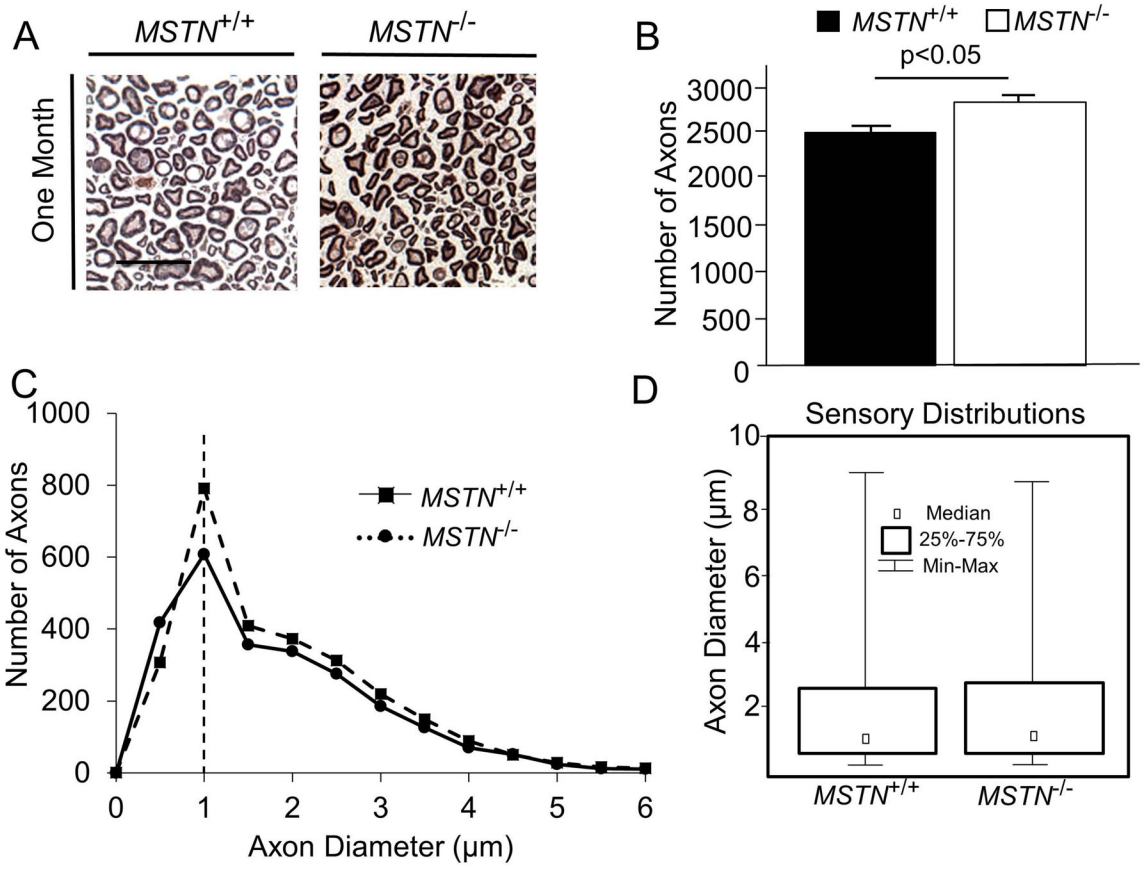

Figure 3. Total numbers and diameters of sensory axons in L5 dorsal roots of *MSTN*$^{+/+}$ and *MSTN*$^{-/-}$ mice

(A) Cross sections of *MSTN*$^{+/+}$ (left) and *MSTN*$^{-/-}$ mice (right) L5 dorsal roots. Scale bar =10 um. (B) Numbers of axons in L5 sensory roots. Counts were averaged from 3 animals for each genotype and analyzed for statistical significance by the student unpaired *t*-test. Sensory axon number was significantly increased in *MSTN*$^{-/-}$ mice. (C) Distribution of sensory axon diameters of *MSTN*$^{+/+}$ and *MSTN*$^{-/-}$ mice. Distribution profiles were similar between *MSTN*$^{+/+}$ and *MSTN*$^{-/-}$ mice. However, the number of axons at 1 μm was increased in *MSTN*$^{-/-}$ mice. (D) Whisker plots of axonal diameter, showing first, second, and third quartile values for *MSTN*$^{+/+}$ (0.6, 1.3, 2.2 μm respectively) and *MSTN*$^{-/-}$ (0.7, 1.3, 2.3 μm respectively) mice. Axonal diameter distribution was analyzed for overall statistical significance using the Mann-Whitney U test. There was a statistically significant difference between diameter distribution of *MSTN*$^{+/+}$ versus *MSTN*$^{-/-}$ mice (P<0.001: N=3)

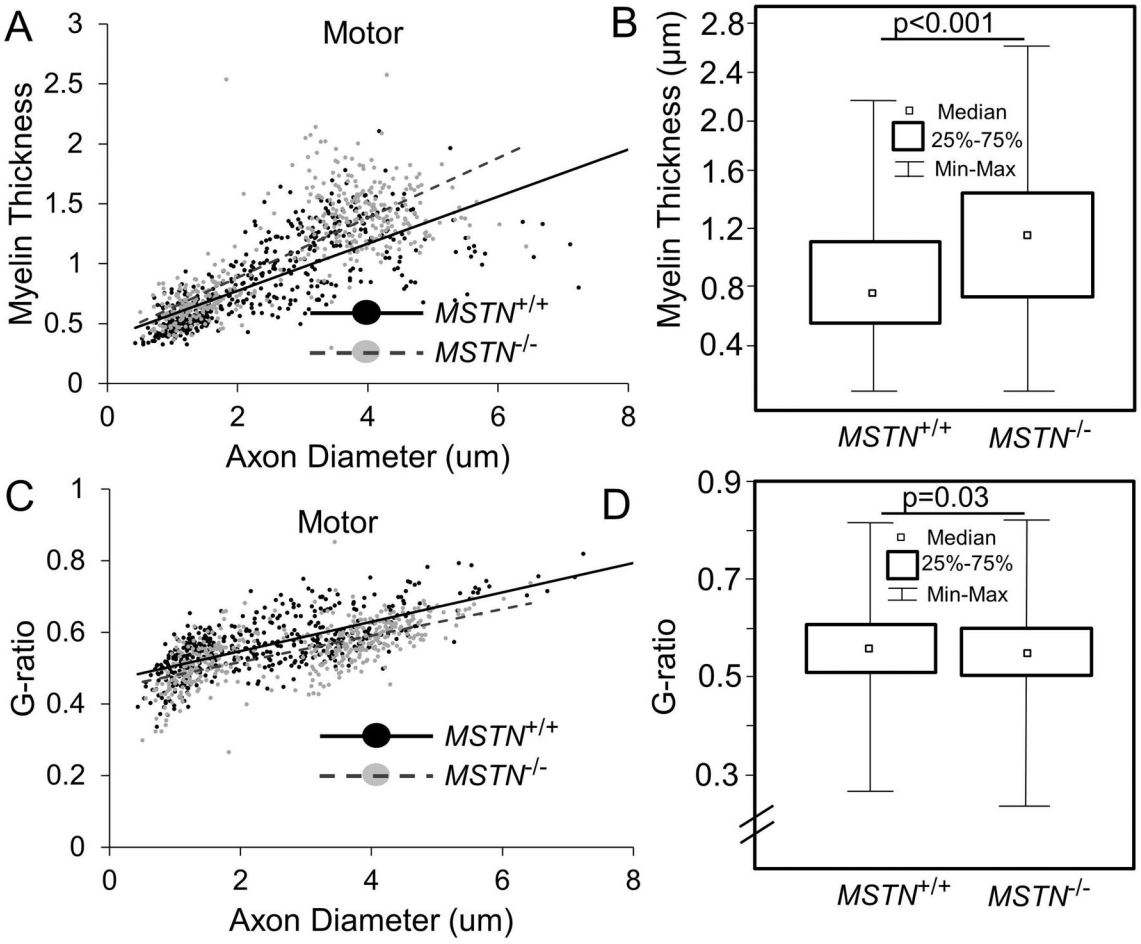

Figure 4. Myelin thickness and g-ratio of motor axons in L5 ventral roots of *MSTN*$^{+/+}$ and *MSTN*$^{-/-}$ mice

(A) Scatter plot of myelin thickness compared to axonal diameter, and (C) g-ratio compared to axon diameter in motor axons from *MSTN*$^{+/+}$ (n=449 axons) and *MSTN*$^{-/-}$ (n=508 axons) mice. Myelin thickness was increased in *MSTN*$^{-/-}$ mice resulting in significantly decreased g-ratios. (B) Whisker plots confirmed the changes in myelin thickness. Myelin thickness whisker plots show first, second, and third quartile values for *MSTN*$^{+/+}$ (0.56, 0.75, 1.15 µm) and *MSTN*$^{-/-}$ (0.67, 1.13, 1.43 µm) mice. (P<0.001). (D) Decreased g-ratio was also confirmed by whisker plot (P=0.03). Myelin thickness and g-ratio were tested for statistical significance using the Mann-Whitney U test (N=3 per genotype).

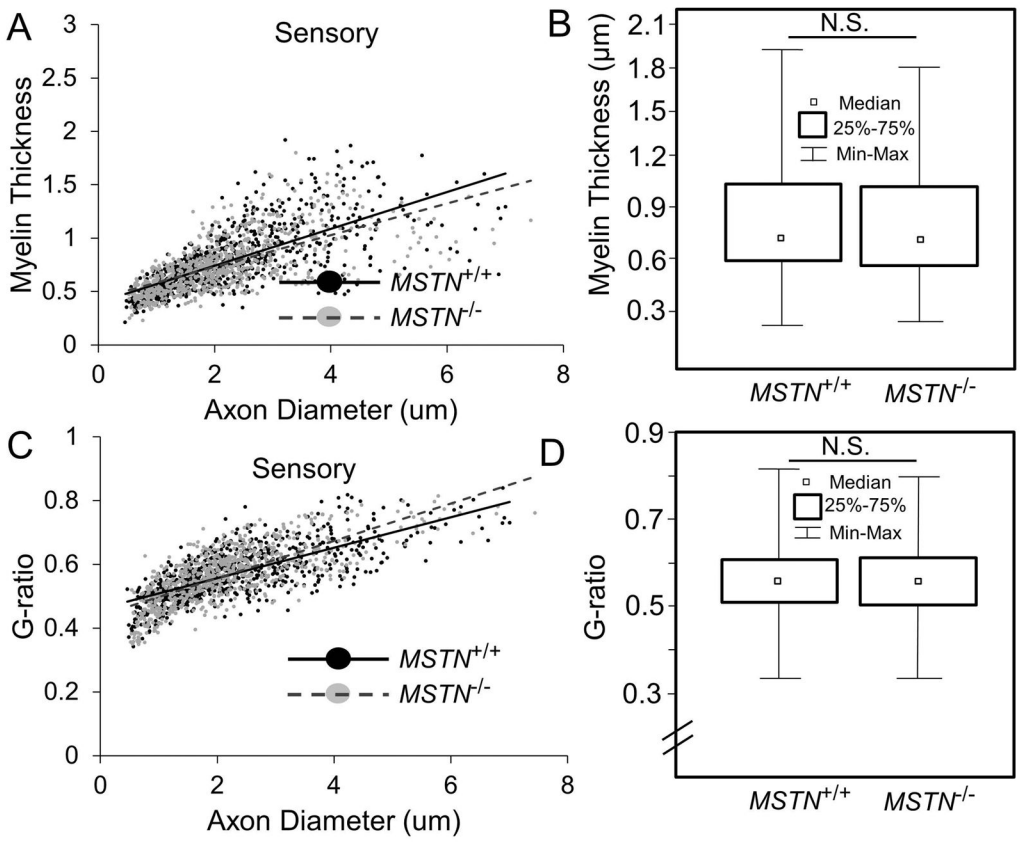

Figure 5. Myelin thickness and g-ratio of sensory axons in L5 dorsal roots of *MSTN*$^{+/+}$ and *MSTN*$^{-/-}$ mice

Scatter plot of myelin thickness compared to axonal diameter (A), and g-ratio compared to axon diameter (C) in sensory axons from *MSTN*$^{+/+}$ (n=751 axons) and *MSTN*$^{-/-}$ (n=750 axons) mice. Myelin thickness and g-ratio were similar in *MSTN*$^{+/+}$ and *MSTN*$^{-/-}$ mice except for the largest diameter sensory axons. (B) Myelin thickness whisker plots show first, second, and third quartile values for *MSTN*$^{+/+}$ (0.58, 0.73, 0.95 µm) and *MSTN*$^{-/-}$ (0.56, 0.71, 0.89 µm) mice. These differences were not statistically significant. (D) Whisker plots of G-ratios also demonstrate no significant differences. Myelin thickness and g-ratio were tested for statistical significance using the Mann-Whitney U test. (N=3 per genotype)

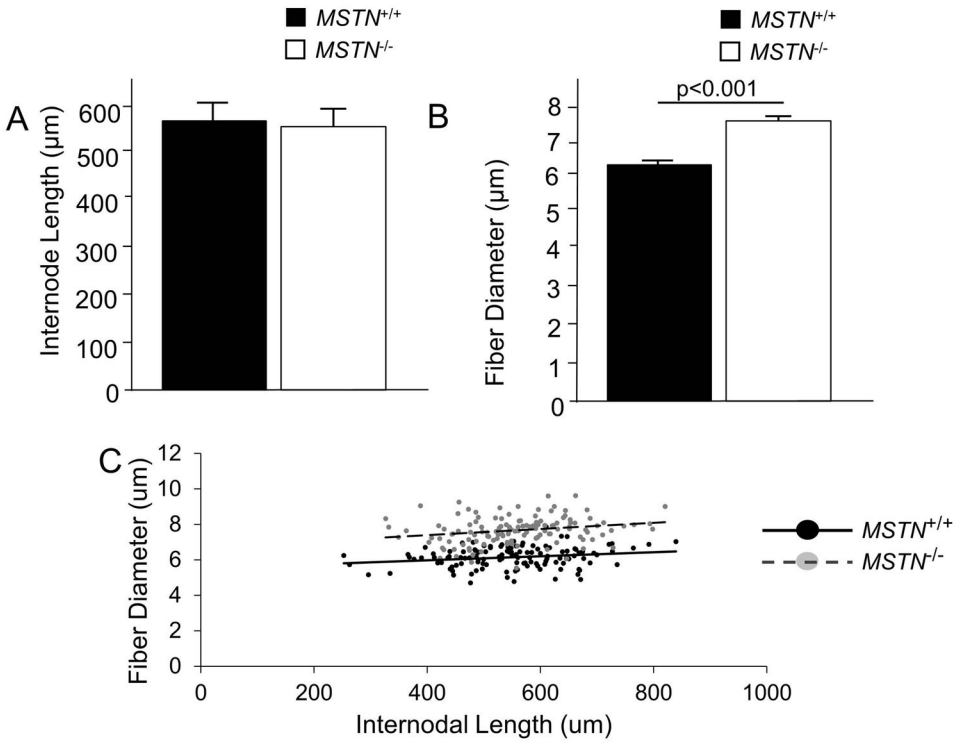

Figure 6. Internode length in L5 ventral roots of *MSTN*$^{+/+}$ and *MSTN*$^{-/-}$ mice

(A). Average internode length was not altered in *MSTN*$^{-/-}$ compared to *MSTN*$^{+/+}$ mice. (B) Average fiber diameter per node was measured, and was significantly (*P*<0.001) increased in *MSTN*$^{-/-}$ mice. The increase in average fiber diameter per internode was similar to the change measured in motor root cross sections (see Figure 1C). (C) Comparing internode length to average fiber diameter per internode demonstrated that internode length did not increase in *MSTN*$^{-/-}$ mice. Internodes within the 400–800µm range were observed for ~6µm axons in *MSTN*$^{+/+}$ mice, whereas the same internode range was observed for axons ~8µm in diameter in *MSTN*$^{-/-}$ mice. Average internode length was analyzed by the student unpaired *t*-test. Error bars = SEM of N= 3 per genotype.

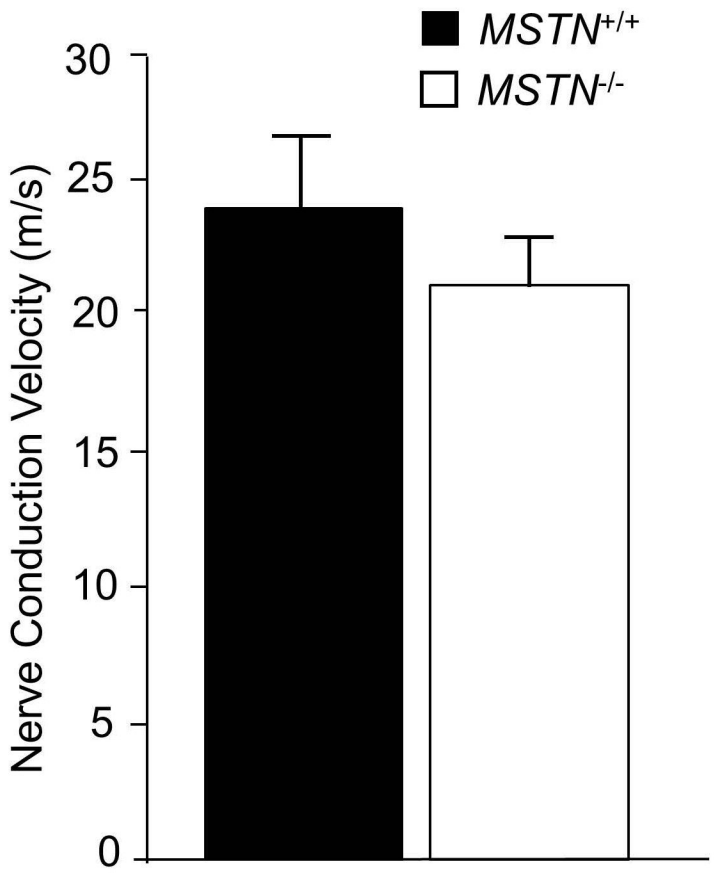

Figure 7. Motor nerve conduction velocity in *MSTN*$^{+/+}$ and *MSTN*$^{-/-}$ mice

Muscle hyperplasia increased axon diameter and myelin thickness in *MSTN*$^{-/-}$ mice without affecting internode length. To determine if these structural alterations affected nerve function, motor nerve conduction velocity (NCV) was measured in *MSTN*$^{+/+}$ and *MSTN*$^{-/-}$ mice. Motor NCV was reduced in *MSTN*$^{-/-}$ mice. However, this difference did not reach statistical significance. Nerve conduction velocities were analyzed by the student unpaired *t*-test. Error bars = SEM of N= 5 per genotype.

Table 1

Binned populations of motor and sensory neurons.

Motor Neurons						
Genotype	**0–1.5 μm**	**>1.5 μm**	**0–2 μm**	**>2 μm**	**Putative γMN**	**Putative αMN**
MSTN$^{+/+}$	363±29	730±26	507±74	586±36	363±29	730±26
MSTN$^{-/-}$	191±22*	805±39	242±15*	754±43*	242±15*	754±43
P-value	**0.006**	0.187	**0.025**	**0.040**	**0.022**	0.662
Sensory Neurons						
Genotype	0–2 μm	>2 μm	0–3 μm	>3 μm	0–4 μm	>4 μm
MSTN$^{+/+}$	1383±103	1102±78	1996±136	489±110	2307±103	178±78
MSTN$^{-/-}$	1508±52	1262±28	2195±55	575±10	2564±55	207±12
P-value	0.337	0.126	0.246	0.479	0.092	0.734

Bold P-values were statistically significant